

RESEARCH ARTICLE

Association of plasma neurofilament light chain with microstructural white matter changes in Down syndrome

Herminia Diana Rosas^{1,2}  | Nathaniel David Mercaldo^{1,2} | Yasemin Hasimoglu^{1,2} |
 Melissa Petersen^{3,4} | Lydia R. Lewis^{1,2} | Florence Lai¹ | David Powell⁵ |
 Asim Dhungana^{1,2} | Ali Demir^{1,2} | David Keater⁶ | Michael Yassa⁷ |
 Adam M. Brickman⁸ | Sid O'Bryant^{3,4}

¹Department of Neurology, Massachusetts General Hospital, Harvard Medical School, Boston, Massachusetts, USA

²Center for Neuroimaging of Aging and Neurodegenerative Diseases, Massachusetts General Hospital, Charlestown, Massachusetts, USA

³Department of Family Medicine, University of North Texas Health Science Center, Fort Worth, Texas, USA

⁴Institute for Translational Research, University of North Texas Health Science Center, Fort Worth, Texas, USA

⁵Magnetic Resonance Imaging and Spectroscopy Center, University of Kentucky, Lexington, Kentucky, USA

⁶Department of Neurobiology and Behavior, University of California, Irvine, California, USA

⁷Department of Psychiatry and Human Behavior, University of California, Irvine, California, USA

⁸Taub Institute for Research on Alzheimer's disease and the Aging Brain Department of Neurology, Vagelos College of Physicians and Surgeons, Columbia University, New York, USA

Correspondence

Herminia Diana Rosas, MGH Department of Neurology, 149 13th Street, Room 10126, Charlestown, Massachusetts, USA.
 Email: hrosas@mgh.harvard.edu

Funding information

National Institutes of Health, Grant/Award Numbers: U01AG051412, U19AG068054, NS106384

Abstract

INTRODUCTION: Both micro- and macrostructural white matter (WM) abnormalities, particularly those related to axonal degeneration, are associated with cognitive decline in adults with Down syndrome (DS) prior to a diagnosis of Alzheimer disease. Neurofilament light chain (NfL) is a support protein within myelinated axons released into blood following axonal damage. In this study we investigated cross-sectional relationships between WM microstructural changes as measured by diffusion tensor imaging (DTI) and plasma NfL concentration in adults with DS without dementia.

METHODS: Thirty cognitively stable (CS) adults with DS underwent diffusion-weighted MRI scanning and plasma NfL measurement. DTI measures of select WM tracts were derived using automatic fiber tracking, and associations with plasma NfL were assessed using Spearman correlation coefficients.

RESULTS: Higher Plasma NfL was associated with greater altered diffusion measures of select tracts.

DISCUSSION: Early increases in plasma NfL may reflect early white matter microstructural changes prior to dementia in DS.

KEYWORDS

Alzheimer's disease, diffusion weighted imaging, Down syndrome, white matter microstructural integrity

Highlights

- The onset of such WM changes in DS has not yet been widely studied.
- WM microstructural properties correlated with plasma neurofilament light chain (NfL).
- NfL may reflect early, selective WM changes in adults with DS at high risk of developing AD.

This is an open access article under the terms of the [Creative Commons Attribution-NonCommercial-NoDerivs](https://creativecommons.org/licenses/by-nc-nd/4.0/) License, which permits use and distribution in any medium, provided the original work is properly cited, the use is non-commercial and no modifications or adaptations are made.

© 2024 The Author(s). Alzheimer's & Dementia: Diagnosis, Assessment & Disease Monitoring published by Wiley Periodicals LLC on behalf of Alzheimer's Association.

1 | INTRODUCTION

Advances in the health care of adults with Down syndrome (DS), one of the most common causes of intellectual disability (ID),¹ has resulted in the life expectancy in DS to exceed 60.² However, by age 40, most adults with DS develop Alzheimer's disease (AD)-related pathology, and many develop clinical symptoms of dementia by age 60.³ The high incidence of AD in people with DS is due to the triplication of the amyloid precursor protein (APP) gene, which is located on chromosome 21. APP causes extracellular deposition of the amyloid beta ($A\beta$) peptide in the form of $A\beta$ plaques⁴, which may accumulate on white matter (WM) fibers or cause stress to surrounding cells and may also be cytotoxic to WM. WM changes play an important role in late-onset AD among neurotypical adults and occur in adults with DS, including in those with mild cognitive impairment (MCI).^{6,7} However, little is known about WM integrity in cognitively stable (CS) adults with DS.

Neurofilament light chain (NfL) is a cytoskeletal protein found within large, myelinated axons in cerebral WM.⁸ It is released into the cerebrospinal fluid (CSF) and blood following axonal damage and can be indicative of neurodegeneration.⁹ Plasma NfL concentration is a potential diagnostic, prognostic, and predictive biomarker for a variety of neurological disorders, including AD.⁹ In DS, plasma NfL may be one of the earliest biomarkers to change before a clinical AD diagnosis, as early as 20 years prior to clinical diagnosis.¹⁰ Plasma NfL concentration also increases at a significantly faster rate in adults with DS than in matched neurotypical adults.¹¹ Increases in plasma and/or CSF NfL concentration can differentiate DS adults with MCI-DS/AD dementia (AD-DS) from those who are CS (ie, individuals without any evidence of cognitive decline).^{12,13} Several studies have found associations between plasma concentration of NfL and indices of WM integrity in other neurodegenerative disorders.^{14,15} However, few studies have focused on individuals without dementia. Such studies could provide important insights into early pathological processes that could herald AD; this possibility is especially true in the DS population, where such associations could provide a strong rationale for early interventions aimed at preventing or delaying onset of AD.

In this study, we evaluated associations between WM microstructure in CS adults with DS and plasma NfL concentrations. We hypothesized that associations between these two measures would be specific to WM tracts we previously identified as selectively vulnerable in CS adults with DS, including the corpus callosum, cingulum, inferior longitudinal fasciculus (ILF), and superior longitudinal fasciculus (SLF).^{6,7} Our findings provide support for widespread changes in WM integrity in CS adults with DS that are associated with elevations in NfL, suggesting that early pathological processes are already under way in CS adults with DS. Moreover, they suggest that early intervention may be necessary to prevent or delay onset of AD in DS.

2 | METHODS

2.1 | Participants

Thirty CS adults with DS and mild to moderate ID from the multi-site Alzheimer's Disease in Down Syndrome (ADDS) study, part of

RESEARCH IN CONTEXT

- 1. Systematic review:** The authors reviewed the literature using traditional (eg, PubMed) sources and meeting abstracts and presentations. White matter (WM) microstructural alterations have been reported in Alzheimer's disease (AD)-related degeneration in adults with Down syndrome (DS). However, the onset of such WM changes in DS has not yet been widely studied.
- 2. Interpretation:** Our findings of WM microstructural properties (including fractional anisotropy, radial diffusivity, axial diffusivity, and mean diffusivity) correlated with plasma neurofilament light chain (NfL) concentrations in cognitively stable (CS) DS adults provide evidence that NfL may reflect early, selective WM changes in adults with DS at high risk of developing AD.
- 3. Future directions:** Longitudinal studies to track progressive WM microstructural changes starting with CS adults with DS could provide a biomarker for early intervention.

the Alzheimer's Biomarker Consortium-Down Syndrome (ABC-DS; <https://www.nia.nih.gov/research/abc-ds>), were included in the analyses. All data were collected using a study-specific code to ensure participant privacy. Clinical status was classified generally consistently with recommendations of the American Association of Mental Retardation- International Association for the Scientific Study of mental Deficiencies (AAMR-IASSID) Working Group for the Establishment of Criteria for the Diagnosis of Dementia in Individuals with Developmental Disability.^{16,17} A CS designation indicated the absence of any clinically significant cognitive decline, confirmed by caregiver reports. Massachusetts General Hospital (MGH), University of California, Irvine, and Columbia University/New York State Institute for Basic Research in Developmental Disabilities served as enrolling sites. Inclusion criteria for the study were as follows: (1) ≥ 40 years of age at baseline, (2) estimated premorbid IQ ≥ 30 , (3) trisomy 21 as confirmed by genetic testing, and (4) English speaker. Participants underwent diffusion-weighted imaging (DWI) and blood collection for plasma NfL concentration measurements.

Consent statement: All procedures were approved by the respective Institutional Review Boards and informed consent and/or assent was obtained for each participant. The work was carried out in accordance with the Declaration of Helsinki.

2.2 | Plasma NfL measurement

Plasma NfL concentrations were measured using a single molecule array (SIMOA) analyzer, as previously described.¹⁸ The lower limit of detection (LLOD) was determined at a concentration of 2.5 standard deviations above the background measurement. For NfL, the LLOD was 0.038 pg/mL and the coefficient of variance was 0.038.

2.3 | MRI acquisition and preprocessing

Scans were acquired at the three sites on Siemens Prisma 3T scanners equipped with the same software using identical protocols and a 32-channel head coil. DWI was performed twice with reversed phase-encoding blips, using a multishell echo-planar imaging protocol (repetition time = 3230 ms, echo time = 89.2 ms, flip angle = 78°, $b = 5, 1500, 3000 \text{ s/mm}^2$, voxel size 1.5 mm^3 isotropic, image matrix size $140 \times 140 \times 92$, field of view $210 \times 210 \text{ mm}$), each producing 92 diffusion-weighted images with seven b_0 images interspersed throughout.

From these pairs of images, the susceptibility-induced off-resonance field was estimated using a method similar to that described in Andersson et al.¹⁹ and as implemented in FSL (<https://fsl.fmrib.ox.ac.uk/fsl/>),²⁰ and the two images were combined into a single corrected one. The eddy tool in FSL was used to correct for eddy current-induced distortions and subject movements²¹ and to detect outlier slices and replace them with non-parametric predictions made by the Gaussian process underlying eddy.²¹

2.4 | Tracts of interest analysis

Eddy-corrected DWI data were uploaded to DSI Studio (<http://dsi-studio.labsolver.org/>) for quality control using exclusion criteria outlined in Yeh et al.²² and subsequent tractography. Neighboring DWI correlation and the number of slices with signal dropout were inspected as measures of quality. Neighboring DWI correlation was calculated as the correlation between DWI volumes with similar gradient direction. The number of slices with dropout was evaluated as a percentage of the total number of slices in the scan (in the present study, $198 \text{ frames} \times 92 \text{ slices per frame} = 18,216 \text{ slices}$). Three participants whose neighboring DWI correlation was less than three median absolute deviations or who had signal dropout in more than 0.1% of the total number of slices (ie, $> 18 \text{ slices}$) were excluded from further analysis.

DWI data were reconstructed in Montreal Neurological Institute (MNI) space using q-space diffeomorphic reconstruction (QSDR) to obtain the spin distribution function (SDF)²³ with a diffusion sampling length ratio of 1.25. Automatic fiber tracking was performed to track the cingulum, corpus callosum, ILF, SLF, corticostriatal, and corticothalamic pathways, using a deterministic fiber-tracking algorithm,²⁴ as these were previously identified as selectively vulnerable in DS. Each subject's quantitative anisotropy (QA) map was normalized to the MNI QA map, and the Human Connectome Project-842 tractography atlas was used to guide track recognition²⁵ and topology-informed pruning to filter out false tracts.²² A seeding region was placed at the pathway of interest and tracking was performed with an anisotropy threshold randomly selected from 0.6 to 0.8 Otsu's threshold, an angular threshold randomly selected from 15° to 90° and step size randomly selected from 0.5 to 1.5 voxels. Tracts with length shorter than 30 or longer than 300 mm were discarded. A total of 10,000 tracts were calculated for each pathway, and the following parameters were extracted from each participant for further statistical analysis: average axial diffusiv-

ity (AxD), which measures diffusion along the preferential direction of diffusion; radial diffusivity (RD), which measures the magnitude of diffusion orthogonal to the preferential direction; fractional anisotropy (FA), which refers to the degree in which there is a preferential direction in the diffusion of water molecules; and mean diffusivity (MD), which refers to the rotationally invariant magnitude of water diffusion within brain tissue values were extracted from each participant for statistical analysis. Higher AxD, RD, MD, and lower FA reflect altered WM microstructural integrity.

2.5 | Positron emission tomography acquisition and analysis

Positron emission tomography (PET) scans were acquired on a Siemens 3T Biograph mMR PET/MRI scanner using a protocol optimized for collection from adults with DS. Approximately 10 mCi of florbetapir was injected and scanning was initiated 50 min after injection and scanning was done for a period of 20 min. Simultaneously collected high-resolution T1-weighted scans were superimposed on the PET scans to achieve co-registration. PET scan reconstruction was performed using a 3D ordinary Poisson ordered subset expectation maximization (3D OP-OSEM) algorithm with attenuation correction.²⁶ Centiloid (CL) values were determined as reported previously.²⁷

2.6 | Statistical analyses

Spearman correlations, their corresponding 95% confidence intervals, and p values were computed to summarize the monotonic association between plasma NfL concentration and each diffusion measure by tract. False discovery rate (FDR)-adjusted p values were computed to account for multiple comparisons. FDR-adjusted p values $< .1$ were considered statistically significant, but values $< .05$ were also highlighted. As a secondary exploratory analysis, we repeated the calculation of the Spearman correlations among subjects with CL values > 20 as a cut-off for amyloid positivity.²⁸ Given the small sample size, p values were omitted from these secondary analyses.

2.7 | Diffusion MRI connectometry

For whole-brain exploratory analysis, diffusion MRI connectometry²⁹ was used to study the association between plasma NfL concentration and diffusion measures using methods outlined by Yeh et al.²³ A T-score threshold of 2.5 was assigned to select local connectomes using a deterministic fiber-tracking algorithm²⁴ to obtain correlational tractography. The tracts were filtered by topology-informed pruning²² with two iterations. A length threshold of 20 mm was used to select tracts showing significant associations with plasma NfL concentration, which was quantified using a permutation test. FDR-adjusted p values were also computed to account for multiple testing.

TABLE 1 Subject Demographics.

Characteristic	Overall (N = 30)
Sex	
Male	18 (60.0)
Female	12 (40.0)
Age	
Median (IQR)	47.0 [43.0, 49.8]
Intellectual disability	
Mild	18 (60.0)
Moderate	12 (40.0)
Plasma NFL	15.3 [12.1, 21.9]
Centiloid	
Median (IQR)	40.5 [6.7, 56.7]
≤20	6 (30.0); 20
>20	14 (70.0); 20

Abbreviations: IQR, interquartile range; NFL, neurofilament light chain.

3 | RESULTS

3.1 | Demographics and participant characteristics

Thirty CS DS subjects were recruited; 12 (40%) were female, 18 (60%) had mild ID, four (13%) were ApoE ε4 positive, and the median (interquartile range [IQR]) age was 47.0 (43.0 to 49.8). All participants had classical trisomy 21. The median (IQR) NFL plasma was 15.3 (12.1, 21.9). CL values were available for 20 subjects; 14 (70%) had a value >20. The demographic traits of the study cohort are presented in Table 1.

3.2 | Correlations with plasma NFL

Table 2 provides the Spearman correlations between tracts of interest and plasma NFL concentration. There were significant positive associations between RD and NFL concentration in all fiber tracts studied. The magnitude of these associations ranged from 0.42 in the corpus callosum to 0.56 in the left (L) cingulum. Similar positive associations were observed between all MD and NFL concentration for all tracts, ranging from 0.37 (L ILF) to 0.53 (L cingulum). Associations between AxD and NFL concentration were observed in all tracts, except L ILF, ranging from 0.33 (L cingulum) to 0.41 right (R) (R corticostriatal). There was an inverse relationship between FA and NFL in all tracts, except L SLF and L corticostriatal, and ranged from −0.34 (L ILF) to −0.51 (L cingulum). Qualitatively, there were no significant hemispheric differences between the tracts from the respective hemispheres.

Among subjects with CL values >20, similar patterns were observed (Table 3). These correlations ranged from 0.38 to −0.56 (AxD), 0.49 to 0.66 (RD), −0.30 to −0.65 (FA), and 0.51 to 0.73 (MD).

3.3 | Connectometry analysis

We performed an exploratory whole-brain analysis to evaluate other potential associations between diffusion measures and NFL concentrations (Figure 1).

We found significant positive associations (FDR < 0.05) between AxD and plasma NFL in bilateral acoustic radiations, bilateral frontal and temporal u-fibers, and R cerebellum, as well as the tracts that we had identified a priori, including bilateral corticothalamic and corticostriatal pathways, corpus callosum, L cingulum, and L SLF (Figure 1A). We also found other significant positive associations between RD and plasma NFL in bilateral parietal and temporal u-fibers, R optic radiation, L arcuate fasciculus, R frontal aslant tract, and R cerebellum (Figure 1B). Significant positive associations between MD and plasma NFL were found additionally in bilateral temporal and parietal u-fibers, R optic radiation, L arcuate fasciculus, L frontal aslant tract, bilateral acoustic radiations, R fornix, and bilateral uncinate fasciculus (Figure 1D). We were unable to detect any inverse correlations between these three measures and plasma NFL. In contrast, we found significant inverse associations between FA and plasma NFL in the R fornix and R cerebellum in addition to the L corticostriatal pathway, bilateral corticothalamic pathways, corpus callosum, and R cingulum (Figure 1C). We were unable to detect any positive correlations between FA and plasma NFL.

4 | DISCUSSION

Our findings support the concept of an important link between alterations in WM integrity and widespread axonal degeneration in CS adults with DS. We demonstrate that WM microstructural properties are associated with axonal degeneration as operationalized by plasma NFL concentration. These results suggest that WM integrity in DS is altered early, before the clinical expression of cognitive deficits associated with AD. Specifically, we found negative correlations between NFL concentration and FA and positive correlations of NFL concentration with AxD, RD, and MD. Associations between diffusion measures and NFL echo previous studies demonstrating that the corpus callosum and limbic pathways (including the fornix) are particularly susceptible to degeneration in presymptomatic autosomal-dominant AD gene carriers,^{30,31} suggesting a parallel between AD-DS and non-DS familial AD. We also found correlations that imply altered integrity in the ILF and SLF, two key late-myelinating pathways. This finding is consistent with the retrogenesis model of AD, which postulates that late-myelinating fibers are more vulnerable to degeneration than early-myelinating fibers³² and builds on existing evidence that early changes in myelin play a key role in DS neuropathology.³³

Associations between the microstructural integrity of the cingulum, which has been shown to be reduced in children with DS,^{7,34} and NFL suggest that there may also be a link between neurodevelopmental alterations and risk of AD pathology. This is supported by our exploratory analyses, which identified associations between diffusion measures and NFL in additional regions. For example, the frontal

TABLE 2 Spearman (ρ) correlations between neurofilament light chain and white matter tract.

Location	AxD		RD		FA		MD	
	ρ (95% CI)	<i>p</i>	ρ (95% CI)	<i>p</i>	ρ (95% CI)	<i>p</i>	ρ (95% CI)	<i>p</i>
Corpus callosum	0.36 (0.00, 0.64)	0.051*	0.42 (0.07, 0.68)	0.022**	-0.35 (-0.63, 0.01)	0.056*	0.41 (0.06, 0.67)	0.024**
L cingulum	0.33 (-0.04, 0.61)	0.078*	0.56 (0.26, 0.77)	0.001**	-0.51 (-0.74, -0.19)	0.004**	0.53 (0.21, 0.75)	0.003**
R cingulum	0.39 (0.04, 0.66)	0.033*	0.52 (0.20, 0.74)	0.003**	-0.42 (-0.68, -0.07)	0.022**	0.49 (0.16, 0.72)	0.006**
L ILF	0.25 (-0.12, 0.56)	0.187	0.42 (0.07, 0.68)	0.022**	-0.34 (-0.62, 0.02)	0.067*	0.37 (0.01, 0.64)	0.046*
R ILF	0.34 (-0.03, 0.62)	0.069*	0.47 (0.13, 0.71)	0.009**	-0.40 (-0.66, -0.05)	0.028*	0.38 (0.02, 0.65)	0.038*
L SLF	0.37 (0.01, 0.65)	0.043*	0.42 (0.07, 0.68)	0.021**	-0.27 (-0.57, 0.10)	0.153	0.43 (0.08, 0.68)	0.019**
R SLF	0.37 (0.01, 0.65)	0.043*	0.44 (0.09, 0.69)	0.015**	-0.38 (-0.65, -0.02)	0.038*	0.45 (0.11, 0.70)	0.012**
L corticostriatal	0.39 (0.03, 0.66)	0.034*	0.44 (0.09, 0.69)	0.016**	-0.31 (-0.60, 0.06)	0.100	0.41 (0.06, 0.67)	0.024**
R corticostriatal	0.41 (0.05, 0.67)	0.026**	0.44 (0.09, 0.69)	0.016**	-0.36 (-0.64, 0.00)	0.052*	0.46 (0.12, 0.71)	0.010**
L corticothalamic	0.39 (0.04, 0.66)	0.031*	0.43 (0.09, 0.69)	0.017**	-0.32 (-0.61, 0.04)	0.080*	0.42 (0.07, 0.68)	0.022**
R corticothalamic	0.38 (0.03, 0.65)	0.037*	0.43 (0.09, 0.69)	0.017**	-0.36 (-0.64, 0.00)	0.051*	0.46 (0.12, 0.70)	0.011**

Note: Reported *p* values denote unadjusted *p* values; FDR-adjusted *p* value < 0.05 are denoted by (*) and < 0.1 (**).
Abbreviations: ILF, inferior longitudinal fasciculus; L, left; R, right; SLF, superior longitudinal fasciculus.

TABLE 3 Spearman (ρ) correlations between neurofilament light chain and white matter tract among subjects with Centiloid > 20 (*n* = 14).

Location	AxD ρ (95% CI)	RD ρ (95% CI)	FA ρ (95% CI)	MD ρ (95% CI)
Corpus callosum	0.50 (-0.04, 0.82)	0.56 (0.04, 0.84)	-0.45 (-0.79, 0.11)	0.59 (0.09, 0.85)
L cingulum	0.41 (-0.16, 0.77)	0.66 (0.19, 0.88)	-0.65 (-0.88, -0.18)	0.73 (0.32, 0.91)
R cingulum	0.47 (-0.08, 0.80)	0.64 (0.17, 0.88)	-0.52 (-0.82, 0.01)	0.61 (0.12, 0.86)
L ILF	0.38 (-0.18, 0.76)	0.55 (0.02, 0.84)	-0.31 (-0.72, 0.26)	0.51 (-0.03, 0.82)
R ILF	0.48 (-0.07, 0.80)	0.61 (0.12, 0.86)	-0.49 (-0.81, 0.05)	0.57 (0.06, 0.85)
L SLF	0.49 (-0.05, 0.81)	0.49 (-0.05, 0.81)	-0.30 (-0.71, 0.28)	0.60 (0.11, 0.86)
R SLF	0.48 (-0.07, 0.81)	0.55 (0.03, 0.84)	-0.49 (-0.81, 0.06)	0.62 (0.13, 0.86)
L corticostriatal	0.50 (-0.04, 0.81)	0.56 (0.04, 0.84)	-0.36 (-0.75, 0.21)	0.56 (0.04, 0.84)
R corticostriatal	0.54 (0.01, 0.83)	0.55 (0.02, 0.84)	-0.46 (-0.80, 0.09)	0.70 (0.27, 0.90)
L corticothalamic	0.50 (-0.04, 0.81)	0.53 (0.00, 0.83)	-0.35 (-0.74, 0.22)	0.56 (0.04, 0.84)
R corticothalamic	0.56 (0.04, 0.84)	0.56 (0.04, 0.84)	-0.46 (-0.80, 0.09)	0.72 (0.30, 0.90)

Note: Given the secondary nature of these analyses and the small sample size, *p* values are not provided.
Abbreviations: ILF, inferior longitudinal fasciculus; L, left; R, right; SLF, superior longitudinal fasciculus.

u-fibers, aslant fibers,³⁵ and arcuate fasciculus are WM tracts that support speech and language and have been shown to predict cognitive decline in the AD spectrum.³⁶ Acoustic radiations, especially in children and adolescents with DS, have been reported to demonstrate early deficits in discrimination and auditory memory.³⁷ The cerebellum is typically hypoplastic in DS but does not typically demonstrate WM alterations until adulthood.³⁸ Abnormalities of the visual cortex have been hypothesized to contribute to the decreased visual acuity experienced by some people with DS³⁹ and may reflect the associations we found in the optic radiations; in addition, the radiations span temporal and parietal cortical areas, areas that demonstrate early and progressive accumulation of amyloid by PET.^{40,41} Further studies are needed to elucidate the contribution of neurodevelopmental abnormalities on neurodegenerative processes in later life.

Greater associations between NFL were also found in individuals who were amyloid positive but CS-, which suggests that A β 1-42-mediated toxicity on myelination may be another driver in the pathological model of early axonal degeneration,^{5,42} or, conversely, myelin dysfunction may drive A β deposition,⁴³ an active area of investigation. Overall, we surveyed pathways from all levels of circuitry. Higher-order association fibers (cingulum, ILF, and SLF), commissural fibers (corpus callosum), and projection fibers (corticostriatal and corticothalamic pathways) all displayed evidence of early axonal damage. Simultaneous correlations of NFL with AxD, RD, MD, and FA suggest that early axonal degeneration may reflect combined pathological processes of demyelination, cerebrovascular disease,⁴⁴ and/or neuronal loss.

Our results build on previous work showing the importance of WM integrity in AD-DS onset and progression and introduce plasma NFL

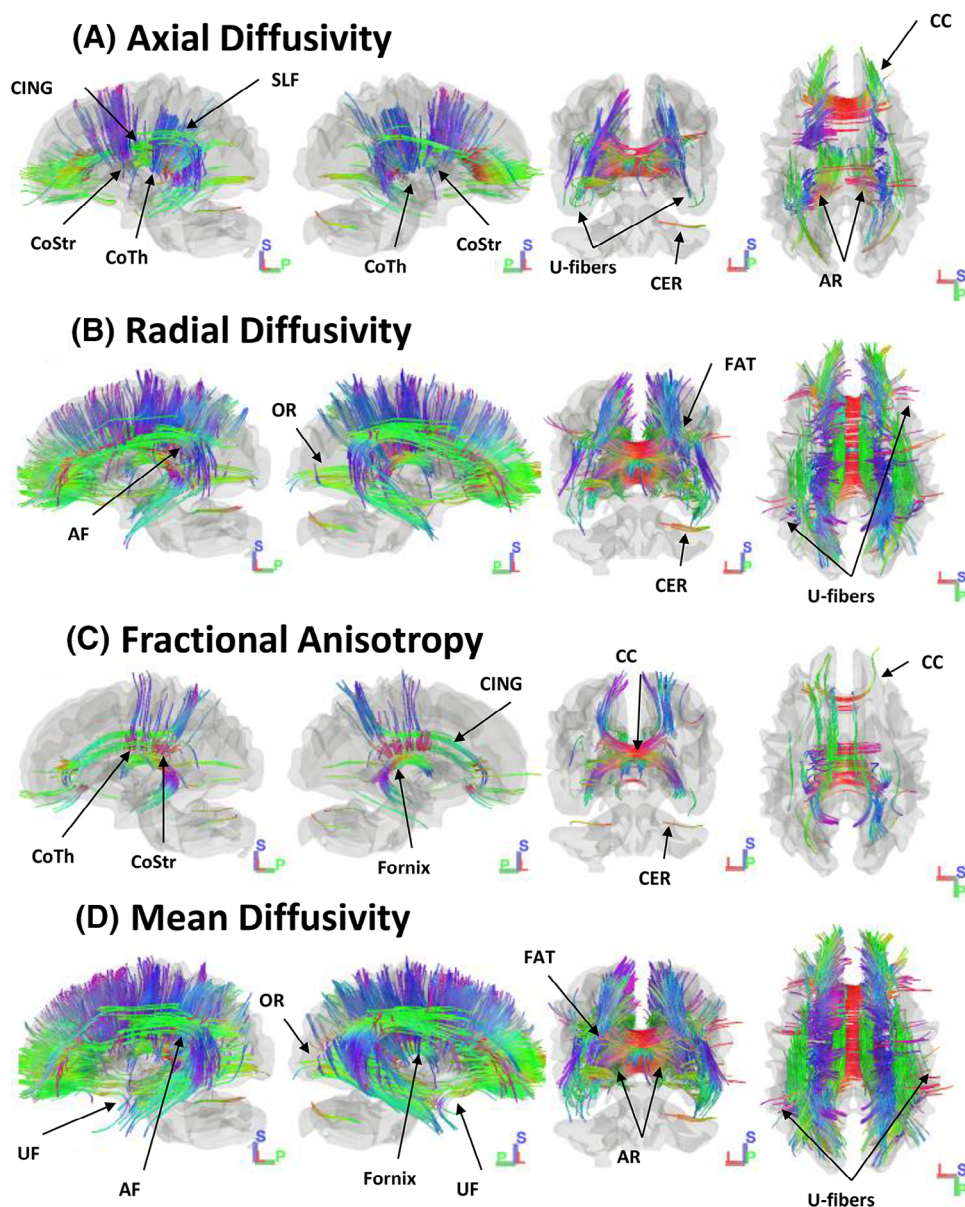


FIGURE 1 Fibers showing positive correlations between plasma NfL and AxD (A), RD (B) and MD (D), and inverse correlation with FA (C). FDR < 0.05 for each. The colors correspond to the direction of the fiber: Red = Left to Right; Green = Anterior to Posterior; Blue = Superior to Inferior. AF, Arcuate fasciculus; AR, Acoustic radiations; CC, Corpus callosum; CER, Cerebellum; CING, Cingulum; CoStr, Corticostriatal; CoTh, Corticothalamic; FAT, Frontal aslant tract; OR, Optic radiation; SLF, Superior longitudinal fasciculus; U-fibers; UF, Uncinate fasciculus.

as a marker that can track neurodegeneration early in DS. We show that early pathology in WM microstructure is already present in non-demented adults. Early interventions targeting WM integrity may be critical for preventing AD in DS.

Fibers showing positive correlations between plasma NfL and AxD (A), RD (B), and MD (D) and an inverse correlation with FA (C). FDR < 0.05 for each. The colors correspond to the direction of the fiber: red = left to right; green = anterior to posterior; blue = superior to inferior. Abbreviations: AR: acoustic radiations; U-fibers; CER: cerebellum; CoTh: corticothalamic; CoStr: corticostriatal; CC: corpus callosum; CING: cingulum; and SLF: superior longitudinal fasciculus;

OR: optic radiation; AF: arcuate fasciculus; FAT: frontal aslant tract; UF: uncinate fasciculus.

ACKNOWLEDGMENTS

The authors are grateful to the individuals who participated in this study and their caregivers who so generously contributed their time and energy to this project and without whom it would not have been possible. The authors also appreciate the efforts of the study teams who helped recruit and assess participants for this study, including Margaret Pulsifer, Sharon Krinsky-McHale, Christy Hom, Courtney Jordan, Eric Doran, Nusrat Jahan, Kelsey Shelofsky, Gabriela Leka,

Gianna Acosta, Eric Doran, Deborah Pang, Tracy Listwan, Cynthia Kovacs. The authors wish to thank Dr. Julie Price for her contributions. The authors thank Howard Andrews for all of his support and his contributions to the curation and maintenance of the study database. The authors also wish to thank Drs. Nicole Schupf, Ira Lott, Wayne Silverman, Ben Handen, Elizabeth Head, Mark Mapstone, and Brad Christian for their encouragement and support of this work. This work was supported by the National Institutes of Health (Grants U19AG068054, U01AG051412, R01 NS026861, R01 NS114562, NS106384). The funding sources were not involved in the conduct of the research and/or the preparation of the article.

CONFLICT OF INTEREST STATEMENT

SEO has multiple patents on precision medicine in neurodegenerative diseases that have been licensed to Cx Precision Medicine and has served on an advisory board for Eisai. DK is employed at the Amen Clinics Inc. and Change Your Brain, Change Your Life foundation. AB receives consulting compensation from Cognition Therapeutics, compensation for serving on the scientific advisory boards of CogState and Cognito Therapeutics, for serving on the data safety monitoring board or advisory board for Albert Einstein College of Medicine and the University of Illinois, Urbana-Champaign, and for serving as section editor for *Alzheimer's & Dementia*, has received honoraria for lectures (Cedara), support from the International Neuropsychological Society to attend meetings, and receives research support from the National Institutes of Health/National Institute on Aging (NIH/NIA). All of the other authors (HDR, NM, YH, MP, LL, FL, DP, AD, AD, and MY) receive support from NIH/NIA but report no other conflicts of interest. Author disclosures are available in the [supporting information](#).

ORCID

Herminia Diana Rosas  <https://orcid.org/0000-0001-9360-7511>

REFERENCES

- Parker SE, Mai CT, Canfield MA, et al. Updated National Birth Prevalence estimates for selected birth defects in the United States, 2004-2006. *Birth Defects Res A Clin Mol Teratol*. 2010;88(12):1008-1016.
- Zigman WB, et al. Alzheimer's disease in adults with down syndrome. *Int Rev Res Ment Retard*. 2008;36:103-145.
- Lai F, Williams RS. A prospective study of Alzheimer disease in Down syndrome. *Arch Neurol*. 1989;46(8):849-853.
- Zigman WB, Lott IT. Alzheimer's disease in Down syndrome: neurobiology and risk. *Ment Retard Dev Disabil Res Rev*. 2007;13(3):237-246.
- Xu J, Chen S, Ahmed SH, et al. Amyloid-beta peptides are cytotoxic to oligodendrocytes. *J Neurosci*. 2001;21(1):RC118.
- Rosas HD, et al. Alzheimer-related altered white matter microstructural integrity in Down syndrome: a model for sporadic AD? *Alzheimers Dement (Amst)*. 2020;12(1):e12040.
- Romano A, Moraschi M, Cornia R, et al. White matter involvement in young non-demented Down's syndrome subjects: a tract-based spatial statistic analysis. *Neuroradiology*. 2018;60(12):1335-1341.
- Moore EE, Hohman TJ, Badami FS, et al. Neurofilament relates to white matter microstructure in older adults. *Neurobiol Aging*. 2018;70:233-241.
- Gaetani L, Salvadori N, Lisetti V, et al. Cerebrospinal fluid neurofilament light chain tracks cognitive impairment in multiple sclerosis. *J Neurol*. 2019;266(9):2157-2163.
- Fortea J, Vilaplana E, Carmona-Iragui M, et al. Clinical and biomarker changes of Alzheimer's disease in adults with Down syndrome: a cross-sectional study. *Lancet*. 2020;395(10242):1988-1997.
- Mengel D, Liu W, Glynn RJ, et al. Dynamics of plasma biomarkers in Down syndrome: the relative levels of Abeta42 decrease with age, whereas NT1 tau and NfL increase. *Alzheimers Res Ther*. 2020;12(1):27.
- Henson RL, et al. Cerebrospinal fluid biomarkers of Alzheimer's disease in a cohort of adults with Down syndrome. *Alzheimers Dement (Amst)*. 2020;12(1):e12057.
- Petersen ME, Rafii MS, Zhang F, et al. Plasma total-tau and neurofilament light chain as diagnostic biomarkers of Alzheimer's disease dementia and mild cognitive impairment in adults with down syndrome. *J Alzheimers Dis*. 2021;79(2):671-681.
- Spotorno N, Lindberg O, Nilsson C, et al. Plasma neurofilament light protein correlates with diffusion tensor imaging metrics in frontotemporal dementia. *PLoS One*. 2020;15(10):e0236384.
- Saraste M, Bezukladova S, Matilainen M, et al. High serum neurofilament associates with diffuse white matter damage in MS. *Neurol Neuroimmunol Neuroinflamm*. 2021;8(1).
- Aylward EH, Burt DB, Thorpe LU, Lai F, Dalton A. Diagnosis of dementia in individuals with intellectual disability. *J Intellect Disabil Res*. 1997. 41(Pt 2):152-164.
- Burt DB, Aylward EH. Test battery for the diagnosis of dementia in individuals with intellectual disability. Working Group for the Establishment of Criteria for the Diagnosis of Dementia in Individuals with Intellectual Disability. *J Intellect Disabil Res*. 2000;44 (Pt 2): 175-180.
- Petersen ME, et al. Plasma total-tau and Neurofilament light chain (Nf-L) as diagnostic biomarkers of Alzheimer's disease dementia and mild cognitive impairment in adults with Down syndrome. *Journal of Alzheimer's Disease*. 2020.
- Andersson JL, Skare S, Ashburner J. How to correct susceptibility distortions in spin-echo echo-planar images: application to diffusion tensor imaging. *Neuroimage*. 2003;20(2):870-888.
- Smith SM, Jenkinson M, Woolrich MW, et al. Advances in functional and structural MR image analysis and implementation as FSL. *Neuroimage*. 2004;23 Suppl 1:S208-S219.
- Andersson JLR, Sotiropoulos SN. An integrated approach to correction for off-resonance effects and subject movement in diffusion MR imaging. *Neuroimage*. 2016;125:1063-1078.
- Yeh F-C, Zaydan IM, Suski VR, et al. Differential tractography as a track-based biomarker for neuronal injury. *Neuroimage*. 2019;202:116131.
- Yeh FC, Tseng WY. NTU-90: a high angular resolution brain atlas constructed by q-space diffeomorphic reconstruction. *Neuroimage*. 2011;58(1):91-99.
- Yeh F-C, Verstynen TD, Wang Y, Fernández-Miranda JC, Tseng W-YI. Deterministic diffusion fiber tracking improved by quantitative anisotropy. *PLoS One*. 2013;8(11):e80713.
- Yeh F-C, Panesar S, Fernandes D, et al. Population-averaged atlas of the macroscale human structural connectome and its network topology. *Neuroimage*. 2018;178:57-68.
- Izquierdo-Garcia D, Chen KT, Hansen AE, et al. New SPM8-based MRAC method for simultaneous PET/MR brain images: comparison with state-of-the-art non-rigid registration methods. *EJNMMI Phys*. 2014;1(Suppl 1):A29.
- Klunk WE, Koeppe RA, Price JC, et al. The Centiloid Project: standardizing quantitative amyloid plaque estimation by PET. *Alzheimers Dement*. 2015;11(1):1-15 e1-4.
- Amadoru S, Doré V, Mclean CA, et al. Comparison of amyloid PET measured in Centiloid units with neuropathological findings in Alzheimer's disease. *Alzheimers Res Ther*. 2020;12(1):22.
- Yeh FC, Badre D, Verstynen T. Connectometry: A statistical approach harnessing the analytical potential of the local connectome. *Neuroimage*. 2016;125:162-171.

30. Ringman JM, O'Neill J, Geschwind D, et al. Diffusion tensor imaging in preclinical and presymptomatic carriers of familial Alzheimer's disease mutations. *Brain*. 2007;130(Pt 7):1767-1776.
31. Araque Caballero MÁ, Suárez-Calvet M, Duering M, et al. White matter diffusion alterations precede symptom onset in autosomal dominant Alzheimer's disease. *Brain*. 2018;141(10):3065-3080.
32. Stricker NH, Schweinsburg BC, Delano-Wood L, et al. Decreased white matter integrity in late-myelinating fiber pathways in Alzheimer's disease supports retrogenesis. *Neuroimage*. 2009;45(1):10-16.
33. Olmos-Serrano JL, Kang HJ, Tyler WA, et al. Down syndrome developmental brain transcriptome reveals defective oligodendrocyte differentiation and myelination. *Neuron*. 2016;89(6):1208-1222.
34. Powell D, Caban-Holt A, Jicha G, et al. Frontal white matter integrity in adults with Down syndrome with and without dementia. *Neurobiol Aging*. 2014;35(7):1562-1569.
35. Hamner T, Udhmani MD, Osipowicz KZ, Lee NR. Pediatric Brain Development in Down Syndrome: A Field in Its Infancy. *J Int Neuropsychol Soc*. 2018;24(9):966-976.
36. Pulsifer MB, et al. Language skills as a predictor of cognitive decline in adults with Down syndrome. *Alzheimers Dement (Amst)*. 2020;12(1):e12080.
37. Gregory L, Rosa RFM, Zen PRG, Sleifer P. Auditory evoked potentials in children and adolescents with Down syndrome. *Am J Med Genet A*. 2018;176(1):68-74.
38. Lee NR, Nayak A, Irfanoglu MO, et al. Hypoplasia of cerebellar afferent networks in Down syndrome revealed by DTI-driven tensor based morphometry. *Sci Rep*. 2020;10(1):5447.
39. Postolache L, Monier A, Lhoir S. Neuro-ophthalmological manifestations in children with down syndrome: current perspectives. *Eye Brain*. 2021;13:193-203.
40. Keator DB, et al., Down syndrome: distribution of brain amyloid in mild cognitive impairment. *Alzheimers Dement (Amst)*. 2020;12(1):e12013.
41. Zammit MD, Tudorascu DL, Laymon CM, et al. PET measurement of longitudinal amyloid load identifies the earliest stages of amyloid-beta accumulation during Alzheimer's disease progression in Down syndrome. *Neuroimage*. 2021;228:117728.
42. Desai MK, Mastrangelo MA, Ryan DA, Sudol KL, Narrow WC, Bowers WJ. Early oligodendrocyte/myelin pathology in Alzheimer's disease mice constitutes a novel therapeutic target. *Am J Pathol*. 2010;177(3):1422-1435.
43. Depp C, Sun T, Sasmita AO, et al. Myelin dysfunction drives amyloid-beta deposition in models of Alzheimer's disease. *Nature*. 2023. 618(7964):349-357.
44. Nasrabady SE, Rizvi B, Goldman JE, Brickman AM. White matter changes in Alzheimer's disease: a focus on myelin and oligodendrocytes. *Acta Neuropathol Commun*. 2018;6(1):22.

SUPPORTING INFORMATION

Additional supporting information can be found online in the Supporting Information section at the end of this article.

How to cite this article: Rosas HD, Mercaldo ND, Hasimoglu Y, et al. Association of plasma neurofilament light chain with microstructural white matter changes in Down syndrome. *Alzheimer's Dement*. 2024;16:e70023.
<https://doi.org/10.1002/dad2.70023>